

A DRIFT CHAMBER TELESCOPE FOR HIGH-Z PARTICLES

J. Isbert,^{1,2} H. J. Crawford,³ T. G. Guzik,¹ M. Hof,²
K. D. Mathis,³ J. W. Mitchell,¹ J. Neuhaus,² M. Simon,² J. P. Wefel,¹

¹Louisiana State University, Baton Rouge, LA USA

²Universitat Siegen, Siegen, West Germany

³Space Sciences Laboratory, Univ. of Calif., Berkeley, CA, USA

Abstract

Drift chambers are one of the position sensing technologies used in cosmic ray balloon and satellite experiments with potential application to the next generation of detectors for space flight. A low mass TPC type drift chamber, employing 8 distinct drift regions within a single gas volume has been built, tested and used at the LBL Bevalac (Hof et al., 1989). From the drift time X-coordinate, spatial resolutions below 100 μm are obtained for a variety of heavy ions with selected trigger modes. The Y-coordinate is determined by pickup pads located behind the anode wire, thereby providing both X and Y coordinates from the same avalanche. Results from different timing schemes, δ -ray effects and the pickup pad resolution are presented.

Experimental Setup: An overall schematic drawing giving the physical dimensions of the drift chamber (DC) telescope is shown in Figure 1. To minimize scattering and interactions, the drift chamber was designed as a single gas volume with only the thin entrance and exit windows and the front and rear potential wires (1 cm spacing) in the path of the particle. This design also gives a very uniform electric field throughout the chamber, but allows only the X coordinate to be measured using drift times. Eight measurement regions, or drift planes, were defined, evenly spaced along the length (Z axis) of the chamber. A mixture of 90% argon and 10% methane was used.

A top view of two of the drift planes giving the relative spacing of the field and sense (anode) wires, along with the sense wire readout scheme, is shown in Figure 2. The mounted sense wire (0.03 mm, gold plated tungsten) were narrowly spaced, each wire having a distance of 6 mm to its neighbors, and were all held at the same voltage. Thus, each wire sampled the ionization along the heavy ion track only over a small region, 3 mm on either side

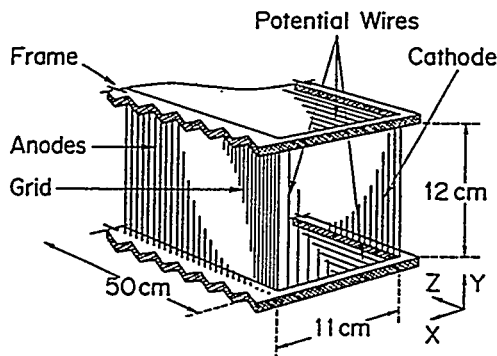


Figure 1: Schematic of the drift chamber

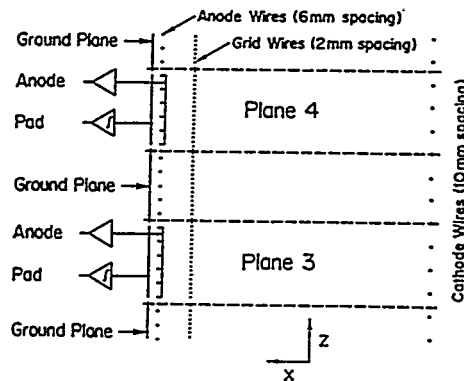


Figure 2: Drift planes (top view)

DISCLAIMER

Portions of this document may be illegible in electronic image products. Images are produced from the best available original document.

of the wire. This arrangement favors short duration signals and a large dynamic range. Six adjacent wires were ganged to form a drift plane, and the combined signal was fed into one preamplifier. The 8 planes were read out in a conventional start and stop technique using a Lecroy 4208 TDC system (24 bit, 1 ns resolution). The stop was derived from the sense wire signal by means of a discriminator. The thresholds of all 8 planes were the same.

The analog electronics for pads and wires were housed in a copper shielded box directly attached to the DC to suppress external noise. We succeeded in operating the whole experimental device in the Bevalac environment with a noise level of 2 mV (rms) following the preamplifiers. A variety of different heavy ions, ranging from nitrogen to iron, were used, and for some runs the DC wire signals were recorded with a high speed waveform digitizer (Lecroy 6880, 1.36 GHz sampling rate). This allowed different timing schemes to be tested as well as the shape of individual wire signals to be analyzed.

Drift Chambers and the δ -ray Problem: Singly charged particles create a low ionization density which influences the timing due to diffusion and clustering (Kobayashi, et al., 1987). The high ionization density in heavy ion tracks reduces these fluctuations, (Schultz et al., 1978) but heavy ions create δ -rays which lead to false stop signals (Simón et al., 1984; 1982).

Figure 3 shows the waveform recorder output for two different sense wire voltages. When the sense wire voltage is high, (bottom picture), a signal is present for the whole drift time, indicating that δ -rays are widely spread in the gas volume. This is most pronounced for iron, and even under these conditions the main peak which belongs to the real iron track is observed clearly above the δ -ray "noise", although it is electronically saturated. With moderate charge amplification (top picture) the δ -ray background is suppressed and the heavy ion is easily detectable. With this arrangement, it is possible to cover the range from nitrogen to iron with the same sense wire voltage.

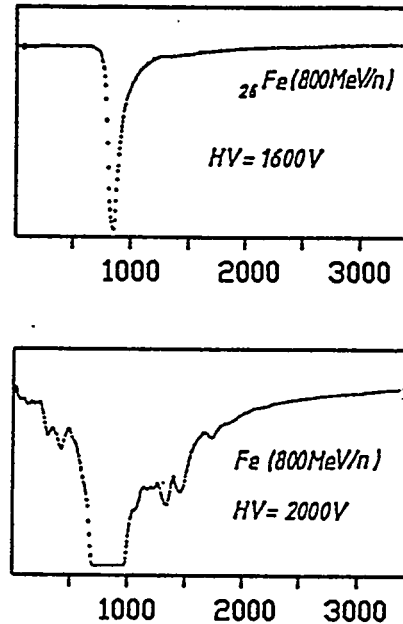


Figure 3: Waveform for ^{56}Fe

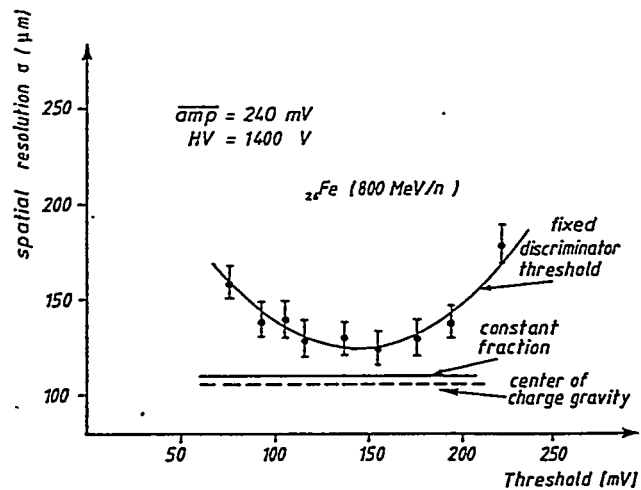


Figure 4: Comparison of timing schemes

Timing Schemes: We compared 3 different timing schemes: Fixed threshold, Constant Fraction and Center-of-Gravity timing. Figure 4 shows these techniques applied to iron particles. Constant fraction timing is performed on the leading edge of the signal, triggering at a certain fraction of the

amplitude, and this compensates for fluctuations in the signal amplitude, improving the overall resolution. For center-of-gravity timing, the mean of the signal between the two FWHM points is calculated and used for analysis. This also improves the spatial resolution over fixed threshold timing and is about equivalent to the constant fraction method.

Y-coordinate: The Y-coordinate was found using an image charge technique measuring the induced charge on pick-up pads, 32 of which were stacked vertically 5 mm behind each set of ganged sense wires. The signal from each pad was amplified and fed into one of a 32 channel sample and hold stage, whose hold signal was derived from the stop signal of the corresponding plane. All 32 sample and hold outputs were fed into a 1 x 32 multiplexer which was read out by a specifically designed microcomputer, which also calculated the center of gravity of the induced charge to get the position of the avalanche along the wire. The Y-computers were read out through the CAMAC readout system of the experiment.

Experiment: The DC-telescope was used in a fragmentation experiment to study the fragmentation of Si at 245 MeV/n, using fixed threshold timing to cover the dynamic range from silicon to beryllium. Figure 5 (top) shows the resolution obtained with this setting for the drift coordinate. The similarity in shape to Figure 4 (fixed threshold) indicates that there is an optimal setting for the threshold relative to the signal amplitude. The bottom plot on Figure 5 shows the resolution for the Y-coordinate, the pads, which is independent of charge over a large range, from silicon to carbon. The reduced resolution for $Z < 6$ is due to limited ADC range.

We also observed space charge effects during this experiment. Due to the much lower ion drift velocity, an additional electric field was created in the direction of the Y-coordinate. This field pointed to the center of the drift chamber, thereby increasing the electron path in the direction and lowering the actual Y-coordinate.

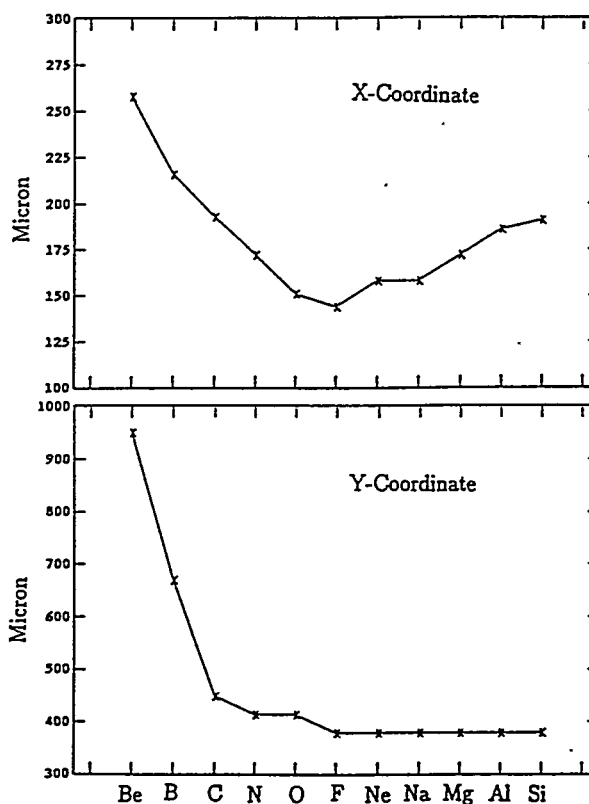


Figure 5: Position resolution versus charge

Conclusion: Drift chambers are capable of measuring heavy ion tracks with a precision better than reported for singly charged particles (Bock et al., 1986). However, to obtain such resolutions, a DC must be operated at moderate charge amplification to avoid δ -ray effects. The fixed threshold results show that there is an optimal setting for the discriminator between about 40 and 60% of the signal amplitude (Hof et al., 1989).

Three different timing techniques have been tested to determine their effects on spatial resolution. Constant fraction and center of gravity timing are both superior to fixed threshold timing. Our results show that drift chambers can give excellent spatial resolution over a wide range in particle charge.

In addition, the charge imaging technique can be used with heavy ions. The pad system gave reasonable spatial resolution, about a factor of three worse than the drift system, but better 0.5 mm.

Acknowledgment: This work has been supported in Germany in part by the DFG and by the BMFT and in the US in part by DOE and in part by NASA.

References:

- Bock, P. et al., 1986, NIM A242, 237.
Hof, M. et al., 1989, NIM A276, 628.
Kobayashi, T. et al, 1987, NIM a254, 281.
Schultz, G. et al., 1978, NIM 151, 413.
Simon, M. et al., 1982, NIM 192, 483.
Simon, M. et al., 1984, NIM 221, 466.

DISCLAIMER

This report was prepared as an account of work sponsored by an agency of the United States Government. Neither the United States Government nor any agency thereof, nor any of their employees, makes any warranty, express or implied, or assumes any legal liability or responsibility for the accuracy, completeness, or usefulness of any information, apparatus, product, or process disclosed, or represents that its use would not infringe privately owned rights. Reference herein to any specific commercial product, process, or service by trade name, trademark, manufacturer, or otherwise does not necessarily constitute or imply its endorsement, recommendation, or favoring by the United States Government or any agency thereof. The views and opinions of authors expressed herein do not necessarily state or reflect those of the United States Government or any agency thereof.